Measurement and *ab initio* calculation of the Ne photoabsorption spectrum in the region of the *K* edge

M. Coreno,[1] L. Avaldi,[1] R. Camilloni,[1] K. C. Prince,[2] M. de Simone,[3] J. Karvonen,[4] R. Colle,[5] and S. Simonucci[6]
[1]*IMAI del CNR, Area della Ricerca di Roma, 00016 Monterotondo, Italy*
[2]*Sincrotrone Trieste, 34012 Trieste, Italy*
[3]*Dipartimento di Fisica ''E. Amaldi,'' III Università di Roma, Roma, Italy*
[4]*Physics Department, University of Oulu, Oulu, Finland*
[5]*Dipartimento di Chimica Applicata, Università di Bologna, 40136 Bologna, Italy and Scuola Normale Superiore, 56100 Pisa, Italy*
[6]*Dipartimento di Matematica e Fisica, Unità INFM, Università di Camerino, Camerino (Mc), Italy*
(Received 1 July 1998; revised manuscript received 18 September 1998)

The Ne photoabsorption spectrum in the region of the *K* edge has been measured with unprecedented energy resolution. The results have been interpreted by using an *ab initio* method that predicts natural linewidths, as well as relative intensities and positions of the different $1s \rightarrow np$ $(3 \leqslant n \leqslant 6)$ transitions. The remarkable agreement between theory and experiment improves the spectroscopic characterization of these inner-shell excited states in an energy region where only electron-energy-loss spectroscopies were considered to provide accurate and high-resolution data. [S1050-2947(99)09002-2]

PACS number(s): 32.70.−n, 32.80.Hd, 32.80.Dz

In the last decade we have witnessed a tremendous improvement in the energy resolution in the vacuum ultraviolet (vuv) and soft x-ray regions. This has been achieved by using new types of monochromators [1,2] at beam lines of synchrotron radiation sources, equipped with undulators and wigglers [3–5]. Due to this improved energy resolution, that is comparable with or even better than the natural width of inner-shell excited states, the spectroscopic information obtained in photoabsorption experiments has significantly superseded the quality of the results of previous high-resolution electron-energy-loss studies [6]. Such detailed studies are now questioning our knowledge of basic quantities, such as, for example, the natural linewidths, and suggest that thorough investigations are needed, where high-resolution experiments and *ab initio* calculations of quantities such as transition energies, natural linewidths, relative intensities, and line shapes are combined. Here we present a study in which the combination of high-resolution experimental data and theoretical values calculated *ab initio* provide an accurate spectroscopic characterization of the region near the Ne *K* edge.

While the energy region up to the nitrogen *K* edge has already been explored at very high resolution [7,8], no comparable results have been previously reported near the Ne *K* edge. Moreover, due to the absence of theoretical predictions of the natural linewidths of the $1s \rightarrow np$ $(n \geqslant 3)$ transitions, reference was made to the measured [9] [0.27(±0.02) eV] and calculated [10] (0.24±10%) natural linewidth of the $Ne^+(1s^{-1})$ state in order to evaluate the resolving power of the different experimental setups. Some confusion on the topic has been generated moreover by the fact that, in the first report of a high-resolution x-ray photoelectron spectroscopy (XPS) spectrum [11], a value of 0.23 eV was incorrectly quoted for this quantity and was later correctly given [9] as 0.27 eV. Furthermore, the low available experimental resolution has caused a large spread in the measured linewidths [4,5,12–19] of the $1s \rightarrow 3p$ transitions, anomalous for such a simple system and definitely larger than the $Ne^+(1s^{-1})$ natural width. On the other hand, the calculated natural linewidth of the ionic state is a semiempirical value obtained by combining Scofield's relativistic relaxed Hartree-Fock calculations of the radiative transition rates [20] and fluorescence yield from the evaluation of Krause [21]. In this paper we calculate *ab initio* natural linewidths, relative intensities, and energies of the *1snp* $(3 \leqslant n \leqslant 6)$ resonant states as well as those of the $Ne^+(1s^{-1})$state using a method specifically developed for studying Auger and autoionization processes in atoms and molecules [22].

The experiments were performed at the gas phase photoemission beam line of the Elettra storage ring. The radiation from a 4.5-m undulator [23] (12.5-cm period) is deflected to the monochromator by a prefocusing mirror that focuses the beam at the entrance slit of the monochromator in the vertical plane and at the exit slit in the horizontal one. The optical concepts of the variable angle spherical grating monochromator [24] as well as the calibration procedure [25] have been described previously. The monochromator consists of two optical elements: a plane mirror and a spherical grating. This design provides the considerable advantage of a fixed focus in the experimental chamber. Five interchangeable gratings cover the energy region 20–1000 eV. In this experiment the fifth grating (1200 lines/mm) has been used. According to the ray tracing and depending on the assumed spot size on the monochromator a resolving power of about 7500 is expected near the Ne *K* edge.

A windowless ionization cell located at the end of the beam line has been used for the photoabsorption experiment. The gas cell is housed in a six-way stainless steel cross mounted on an $x-y$ manipulator to enable easy alignment on the incident beam direction. Two plates 100 mm long and 20 mm wide are used to collect ions (electrons, depending on the bias voltage) produced by the interaction of the incident radiation with the target gas. During the present experiment the cell was operated typically at a bias voltage of 30 V and at a pressure of 5×10^{-2} mbar. A 2-mm bore and 5-mm-long pipe in front of the six-way cross acts as a first differential pumping section, resulting in a pressure drop of about a fac-

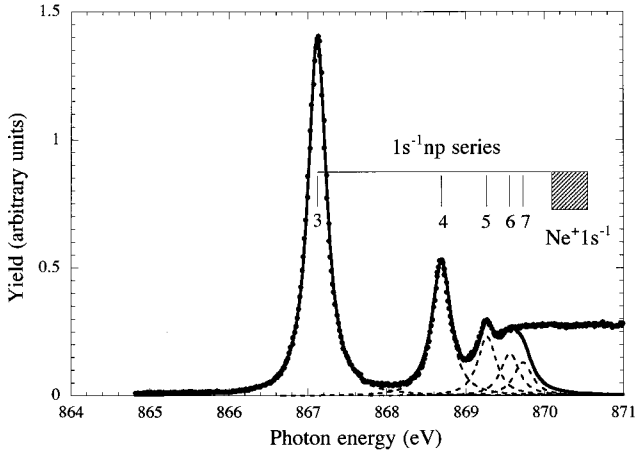

FIG. 1. Ne photoabsorption spectrum in the region of the K edge; the contributions of the different $1s \rightarrow np$ transitions obtained by the best-fit procedure are shown.

tor of 100 between the cell and the $x-y$ manipulator. A photodiode (International Radiation Detectors Ltd. type AXUV-100) located at the exit of the gas cell was used to monitor the flux of the incident photon beam and to ensure that the photoion spectra were collected in the linear absorption regime. A Macintosh Centris computer with a Labview code was used to set the photon energy and to record synchronously the ionization current and beam monitor signal.

The results of the experiments obtained at the first diffraction order and with both the slits set at 10 μm are shown in Fig. 1. The $1s \rightarrow 3p,4p,5p$ transitions are clearly discerned in the spectrum. The $1s \rightarrow 6p,7p$ transitions have been located with the help of the Rydberg formula with the $Ne^+(1s^{-1})$ ionization potential set at 870.17 eV [26,17].

The energy calibration of the grating has been achieved using the O_2 $1s \rightarrow \pi^*$, Xe $3d \rightarrow 6p$, and Ne $1s \rightarrow 3p$ transitions to obtain the settings of the plane mirror which minimize the defocusing term and give the best resolution [25]. A numerical solution of a mathematical model of the monochromator gives the settings for the plane mirror and gratings and provides the working conditions for any energy in the range. During the measurement the plane mirror is held fixed and only the grating is scanned.

In a first analysis of the data no attempt was made to deconvolve the raw data to extract the natural linewidth and the experimental contribution. We have only looked for a suitable representation of the data to extract the overall width of peaks in Fig. 1. Consistent results are obtained by fitting either a Voigt line shape or the Pearson7 function proposed by Krause and Caldwell [27]. The derived full width at half maximum (FWHM) for the $1s \rightarrow 3p$ resonance is 278 ± 5 meV. This value represents a definite improvement when compared with the values of the same quantity as reported in the literature [4,5,12–19], that spread between 670 ± 30 meV [12] and 290 meV [5], the latter obtained by Larsson *et al.* at second diffraction order. By using the second diffraction order the FWHM of the $1s \rightarrow 3p$ resonance measured in this work reduces to 268 ± 5 meV. This result does not represent a noticeable improvement, thus the following discussion will be based on the results obtained at the first diffraction order.

The transition energies measured in the present work are in good agreement with previous determinations [15,17,26,28]. They are reported in the last column of Table I, where only the statistical uncertainty from the best-fit procedure is quoted. A systematic contribution due to the uncertainties of the reference transitions used for the calibration has also to be accounted for. This will result not only in an uncertainty in the absolute energy, but also in a compression/dilatation of the scale. We have calculated, using the two extreme values quoted in the literature for the Ne $1s \rightarrow 3p$ resonance [15,17], that this latter effect results in a difference of 10 meV in the relative position of the *1s3p* and *4p* resonances.

General agreement exists among the different measurements reported in the literature, although the relative position of the $1s \rightarrow 3p$ and *4p* resonances measured here seems to be slightly smaller than in all the previous measurements.

The natural lifetimes of the *1snp* ($3 \leqslant n \leqslant 6$) resonances, as well as their intensities and positions, have been calculated using the theoretical method summarized in the following.

The structures observed in the photoabsorption and emission spectra of light atoms excited by nearly monochromatic incident light in the region below an inner-shell ionization threshold are due to autoionization processes. In this type of non-radiative decay processes one electron is ejected into a specific channel that belongs to a set of different continua which embed quasibound states (resonances) of the neutral target. Interference effects between direct ionization and resonant paths are thus a peculiar feature of this type of spectrum.

The theoretical interpretation of these spectra follow Fano's method [29] for the interaction between discrete and

TABLE I. Natural widths (Γ), calculated (E_n^{calc}) and measured (E_n^{expt}) energies of the resonances 1*snp* ($3 \leqslant n \leqslant 7$) and of the core-hole state $Ne^+(1s^{-1})$. The first term of the second and third columns gives the value calculated using the optimized basis set, while the second term is the average of the results obtained with three different basis sets of Gaussian functions. The estimated uncertainties are given in brackets.

	Γ (meV)			E_n^{calc} (eV)			E_n^{expt} (eV)	
1s3*p*	259	254	($\pm$20)	867.14	867.12	($\pm$0.03)	867.12	($\pm$0.05)
1s4*p*	252	246	($\pm$20)	868.73	868.71	($\pm$0.03)	868.69	($\pm$0.04)
1s5*p*	254	250	($\pm$20)	869.31	869.29	($\pm$0.03)	869.27	($\pm$0.05)
1s6*p*	255	249	($\pm$20)	869.58	869.56	($\pm$0.03)	869.56[a]	
1s7*p*							869.73[a]	
$Ne^+(1s^{-1})$	276	271	($\pm$20)	870.12	870.07	($\pm$0.06)	870.17[b]	

[a]Determined with the Rydberg formula.
[b]From Refs. [26], [17].

continuum states. The general theory, including also the effects due to the finite resolution of the monochromator, can be found in Ref. [30], and in Ref. [31] for its application to the case of an isolated resonance with natural width Γ and energy position E_r. Here we give only the final expression used for calculating the total emission rate $W^{\lambda}_{0\to\alpha}(\omega,\gamma)$ of a photoionization process in which the target in its ground state $|0\rangle$ is ionized to a final state $|\alpha\rangle$ by linearly polarized (λ) radiation having a spread γ around a given frequency ω:

$$W^{\lambda}_{0\to\alpha}(\omega,\gamma)=\frac{N\omega^3}{2\pi c^3}\{D^{\mathrm{dir}}_{\alpha,\lambda}+[\sqrt{(2\pi)}/\gamma]\times[A_{\alpha,\lambda}V_0(x,a)+B_{\alpha,\lambda}V_1(x,a)]\},$$
$$x=(E_r-\omega)/\gamma\sqrt{2},\quad a=\Gamma/\gamma\sqrt{8}. \tag{1}$$

In Eq. (1) $V_0(x,a)$ and $V_1(x,a)$ are, respectively, the standard Voigt function and its complementary part [31], N is a dimensionless scale factor, and $D^{\mathrm{dir}}_{\alpha,\lambda}, A_{\alpha,\lambda}, B_{\alpha,\lambda}$ give the contributions, respectively, of the direct and resonant photoionization paths and of their interference. (For the analytic expressions of these terms see Ref. [31]). The total photoabsorption spectrum is obtained by adding as many terms $W^{\lambda}_{0\to\alpha}$ as final states of the ionized target are taken into account.

For calculating the scattering wave function necessary to evaluate the above spectroscopic terms we have used a method [32] based on the separation of the electronic Hamiltonian into a zero order operator having a continuous spectrum (the kinetic energy operator) and a nonlocal perturbation (the potential energy operator) represented in terms of a finite number *(m)* of Gaussian functions $\{g_j\}$ as follows:

$$\hat{H}(1,\ldots,N)=\hat{T}(1,\ldots,N)+\hat{V}_{\pi}(1,\ldots,N),$$
$$\hat{V}_{\pi}=\sum_{i=1}^{N}\hat{\pi}(i)\hat{v}^{en}\hat{\pi}(i)+\tfrac{1}{2}{\sum_{i,j=1}^{N}}'\hat{\pi}(i)\hat{\pi}(j)\hat{v}^{ee}\hat{\pi}(i)\hat{\pi}(j),$$
$$\hat{\pi}=\sum_{j}^{m}|g_j\rangle\langle g_j|, \tag{2}$$

where $\hat{v}^{en}$ and $\hat{v}^{ee}$ are the standard monoelectronic and bielectronic contributions to the potential energy operator. The Schrödinger equation for the N-particle stationary state, calculated at the energy $E=E_{\alpha}+k^2/2$, is solved inside a finite space of M antisymmetrized products of the following type:

$$\Phi_{\alpha\vec{k}}(1,\ldots,N-1,N)=\sqrt{N}\hat{\mathcal{A}}[\Theta_{\alpha}(1,\ldots,N-1)\varphi_{\alpha\vec{k}}(N)], \tag{3}$$

where $\hat{\mathcal{A}}$ is the antisymmetrizer between the state $|\Theta_{\alpha}\rangle$ of the ionized target with energy E_{α} and the spin orbital $\varphi_{\alpha\vec{k}}=\eta_{\vec{k}}\sigma_{\alpha}$ of the unbound electron. The spatial part $\eta_{\vec{k}}$ of the spin orbital is taken as eigenfunction of the kinetic energy operator $(\hat{p}^2/2)$ in a space orthogonal to the occupied orbitals $\{\theta_j\}$ of the $\{\Theta_{\alpha}\}$ states:

$$(\hat{1}-\hat{P})(\hat{p}^2/2)(\hat{1}-\hat{P})\,\eta_{\vec{k}}=(k^2/2)\,\eta_{\vec{k}},\quad \hat{P}=\sum_{j}^{\mathrm{occ}}|\theta_j\rangle\langle\theta_j|. \tag{4}$$

One can prove [32] that the required scattering rate $|\psi^{-}_{\alpha\vec{k}}\rangle$, with the appropriate ingoing wave boundary condition $(-)$, has the following structure:

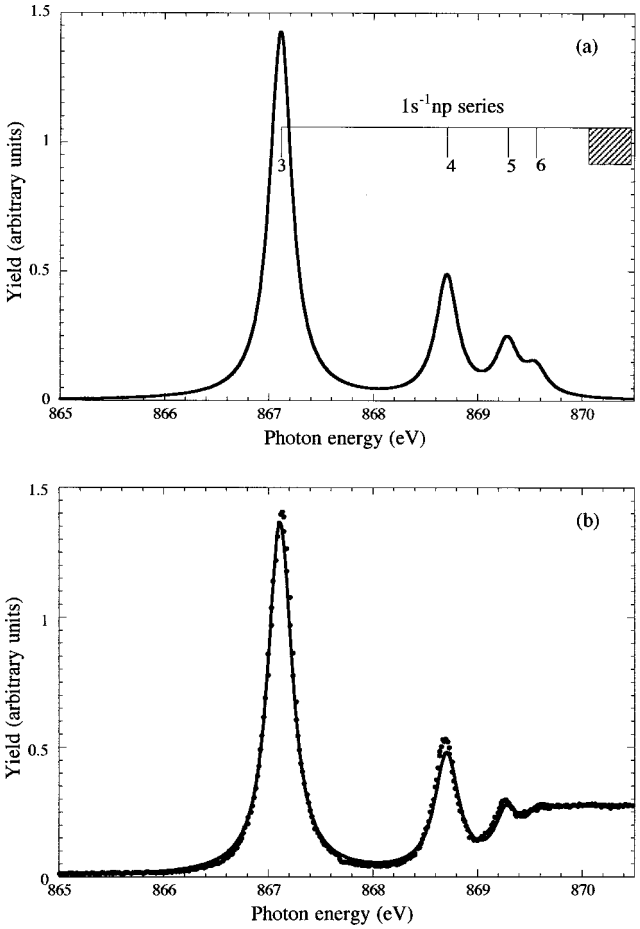

FIG. 2. (a) The theoretical spectrum calculated with $\gamma=0$ and without the contributions of the 1*s* ionization. (b) Comparison between the experimental (dots) and theoretical (continuous line) spectrum calculated with $\gamma=31$ meV and including the contributions of the 1*s* ionization.

$$|\psi^{-}_{\alpha\vec{k}}(E)\rangle=|\Phi_{\alpha\vec{k}}\rangle+\hat{G}^{-}_{0}(E)\hat{\mathcal{T}}|\Phi_{\alpha\vec{k}}\rangle, \tag{5}$$

with

$$\hat{G}^{-}_{0}(E)=\lim_{\nu\to 0}\sum_{\beta}^{M}\int\frac{|\Phi_{\beta\vec{p}}\rangle\langle\Phi_{\beta\vec{p}}|}{(E-i\nu)-(E_{\beta}+p^2/2)}d\vec{p} \tag{6}$$

and

$$\hat{\mathcal{T}}=\hat{V}[1/\hat{V}-\hat{V}\hat{G}^{-}_{0}(E)\hat{V}]\,\hat{V}. \tag{7}$$

The transition operator $\hat{\mathcal{T}}$ is defined in terms of the effective potential $\hat{V}$. The explicit expression of $\hat{V}$ is given in Ref. [32].

The calculations have been performed using three different sets of Gaussian functions in order to find the basis set dependence of the matrix elements characteristic of the problem and to evaluate the resulting uncertainty in the calculated spectroscopic quantities. In Table I we give natural widths (Γ) and energies of the resonances 1*snp* ($3\leqslant n\leqslant 6$) and of the core-hole state $Ne^{+}(1s^{-1})$ calculated using a set of Gaussian functions optimized according to the procedures of Ref. [32]. This optimized basis set consists of 26 *s*-type functions ($\alpha_{\max}=42\,082.18$, $\alpha_{\min}=0.001\,451$), 20 *p*-type functions ($\alpha_{\max}=141.4488$, $\alpha_{\min}=0.000\,993$), and eight *d*-type functions ($\alpha_{\max}=34.9012$, $\alpha_{\min}=0.210\,92$). In Table I we give also the average values and the uncertainties of the

spectroscopic quantities calculated using the three different basis sets and, in the last column, the resonance energies measured in this work.

The results of Table I show that the calculated natural linewidth of the core-hole state $Ne^+(1s^{-1})$ agrees precisely with the corresponding value of $0.27(\pm 0.02)$ eV deduced from the experiment [9]. The calculated change of the natural linewidths of the resonances with the principal quantum number n is below the limit of accuracy of the method and, therefore, is not discussed here. The natural linewidths of the resonances are about 6–8 % smaller than that of the $Ne^+(1s^{-1})$state. This is consistent with previous calculations on molecules [33] and solids [34], where the presence of a spectator electron produced by the primary excitation increases the lifetime of the intermediate quasibound state.

The calculated transition energies reported in Table I are all shifted by 1.04 eV for a better comparison with the experimental values of the last column. This uniform shift, that does not alter the relative positions of the resonances, accounts for the errors due to the finite dimension of the basis set used for the representation of the orbitals, to the finite number of configurations used in the expansion of the states and to the neglect of the relativistic effects. The extension of the basis set and of the configuration space can reduce the size of this energy shift, but only slightly changes the relative positions of the resonances that already agree very well with the experiment.

In Fig. 2 the experimental results and the theoretical spectrum, obtained by superimposing the emission rates calculated for several different final states of the ion, are compared. In particular, Fig. 2(a) shows only the theoretical spectrum calculated assuming monochromatic incident light and including only the contributions of the transitions up to $n=6$. In Fig. 2(b) the theoretical spectrum includes also the contribution of the 1*s* ionization (evaluated using the analytic expression of Ref. [15]) and takes into account the finite resolution of the monochromator. For the purpose we have used the parameter γ of Eq. (1) as a free parameter in a least-squares procedure. The best fit is obtained with $\gamma=31$ meV. Such a value corresponds to incident light with a spread in energy described by a Gaussian with a FWHM of 73 meV, a width definitely smaller than the natural widths of the states in the region of the Ne *K* edge. The determined FWHM corresponds to a resolving power larger than 11 000, better than that estimated, but consistent with the performances of the monochromator obtained at lower photon energies [25].

The agreement between the theoretical predictions and the experimental spectrum is very satisfactory, both as far as the relative intensities and the energy positions of the resonances are concerned. On the other hand, the experimental results clearly show that, also in the case of the Ne inner-shell excited states, the achievable energy resolution at third generation radiation sources is definitely better than the natural linewidths of the resonances.

The combination of experimental results and *ab initio* calculations has provided new and accurate values of the main spectroscopic quantities characteristic of the Ne inner-shell excited states. Similar exercises, when repeated on inner-shell excited states of more complex atomic targets and molecules, are expected to improve the current state of spectroscopic characterization of the inner-shell excited states.

We thank our colleagues at Elettra for their help and support. In particular, we would like to thank L. Romanzin and G. Sandrin for their technical assistance, and M. Vondracek for the energy calibration computations.

[1] C. T. Chen, Nucl. Instrum. Methods Phys. Res. A **265**, 595 (1987).
[2] H. Petersen, Opt. Commun. **40**, 402 (1982).
[3] C. T. Chen and F. Sette, Rev. Sci. Instrum. **60**, 1616 (1988).
[4] M. Domke *et al.*, Rev. Sci. Instrum. **63**, 80 (1992).
[5] C. U. S. Larsson *et al.*, Nucl. Instrum. Methods Phys. Res. A **337**, 603 (1994).
[6] C. G. King and F. H. Read, in *Atomic Inner Shell Physics*, edited by B. Crasemann (Plenum, New York, 1985), p. 317, and references therein.
[7] Y. Ma *et al.*, Phys. Rev. A **44**, 1848 (1991).
[8] C. Quaresima *et al.*, Nucl. Instrum. Methods Phys. Res. A **436**, 374 (1995).
[9] S. Svensson *et al.*, Phys. Scr. **14**, 141 (1976).
[10] M. O. Krause and J. H. Oliver, J. Phys. Chem. Ref. Data **8**, 329 (1979).
[11] U. Gelius *et al.*, Chem. Phys. Lett. **28**, 1 (1974).
[12] D. V. Morgan *et al.*, Phys. Rev. A **55**, 1113 (1997).
[13] J. E. Rubensson *et al.*, Chem. Phys. Lett. **257**, 447 (1996).
[14] L. Avaldi *et al.*, Phys. Rev. A **51**, 5025 (1995).
[15] C. M. Teodorescu *et al.*, J. Phys. B **26**, 4019 (1993).
[16] A. Yagishita *et al.*, Rev. Sci. Instrum. **63**, 1351 (1992).
[17] A. P. Hitchcock and C. F. Brion, J. Phys. B **13**, 3269 (1980).
[18] D. Cvetko *et al.*, in *Gratings and Grating Monochromators for Synchrotron Radiation*, edited by W. McKinney and C. Palmer, SPIE Proceedings Series Vol. 3150 (Palmer Editors, San Diego, California, 1997), p. 86.
[19] M. Watanabe *et al.*, in *Gratings and Grating Monochromators for Synchrotron Radiation* (Ref. [18]). p. 58
[20] J. H. Scofield, in *Atomic Inner Shell Processes*, edited by B. Crasemann (Academic, New York, 1975), Vol. I, pp. 265–288.
[21] M. O. Krause, J. Phys. Chem. Ref. Data **8**, 301 (1979).
[22] R. Colle and S. Simonucci, Phys. Rev. A **48**, 392 (1993), and references therein.
[23] B. Diviacco *et al.*, Rev. Sci. Instrum. **63**, 388 (1992).
[24] P. Melpignano *et al.*, Rev. Sci. Instrum. **66**, 2125 (1995).
[25] K. C. Prince *et al.*, J. Synchrotron Radiat. **5**, 565 (1998).
[26] F. Wuileumier, C. R. Seances Acad. Sci., Ser. B **270**, 825 (1970).
[27] M. O. Krause and C. D. Caldwell, in *VUV and X-ray Photoionization*, edited by U. Becker and D. A. Shirley (Plenum, New York, 1996), p. 181.
[28] J. M. Esteva *et al.*, J. Phys. B **16**, L263 (1983).
[29] U. Fano, Phys. Rev. **124**, 1866 (1961).
[30] R. Colle and S. Simonucci, Mol. Phys. **92**, 409 (1997).
[31] R. Colle and S. Simonucci, Nuovo Cimento D **1**, 705 (1998).
[32] R. Colle and S. Simonucci, Phys. Rev. A **42**, 3913 (1990).
[33] R. Colle and S. Simonucci, Nuovo Cimento D **14**, 705 (1992).
[34] G. Strinati, Phys. Rev. Lett. **49**, 1519 (1982); Phys. Rev. B **29**, 5718 (1984).